Angle-resolved photoemission studies of a surface state on a stepped Cu(332) surface

A. P. Shapiro,* T. Miller, and T.-C. Chiang
Department of Physics and Materials Research Laboratory, University of Illinois at Urbana-Champaign, Urbana, Illinois 61801
(Received 16 July 1987)

A surface state on a stepped Cu(332) surface is studied by angle-resolved photoemission. Based on high-energy electron-diffraction patterns, the (332) sample consists of fairly regularly spaced Cu(111) terraces, which have the form of a strip with a width of about 5–6 atomic rows (about 12 Å). The measured dispersion of the surface state is significantly different from that of the corresponding (111) surface state. Thus, the (332) surface state is delocalized within the surface plane, and the lateral coherence length of the wave function is larger than the terrace width. The dispersion shows a maximum binding energy at the surface Brillouin-zone boundary.

I. INTRODUCTION

In this paper, we report an angle-resolved photoemission study of a surface state on a stepped surface, Cu(332). A stepped surface is slightly tilted relative to a surface with low Miller indices;[1] in the present case, Cu(332) makes an angle of 10.02° relative to Cu(111). The (111) surface of a fcc crystal consists of atoms arranged in a planar hexagonal close-packed pattern, and is a very stable surface due to the high areal atomic density. A vicinal surface slightly tilted relative to the (111) surface usually consists of (111) terraces and atomic steps. For the Cu(332) surface, the terraces have the form of a strip with a width on the average about 5–6 atomic rows due to the 10° tilt.

The Cu(111) surface is known to have an occupied surface state band around the surface Brillouin-zone center.[2–6] It is located within a bulk band gap at the L point in the bulk Brillouin zone; therefore, this surface state is commonly referred to as the L-gap surface state. The question to be discussed here is what would happen to the (111) surface state when atomic steps are introduced on the (111) surface to form a (332) surface.

If the surface-state wave functions associated with different (111) terraces on the (332) surface can be considered as independent, then each terrace should support the same (111) surface state, possibly slightly broadened due the finite size of the terraces. This could happen if the step edges simply act as incoherent scattering centers. On the other hand, if the terrace structure is regular (periodic), the surface-state wave functions associated with neighboring terraces can interact coherently to give rise to interference effects. If this happens, the (332) surface state will show a different energy-momentum relationship than the (111) surface state. The question about the degree of independence depends on the lateral coherence length of the surface state under consideration as well as the degree of ordering of the terrace structure. The latter factor would depend on the manner in which the sample is prepared.

The present experiment measures the band dispersion of this Cu(332) surface state, and finds that the dispersion is distinctly different from the (111) case. The result shows that the terrace structure on our (332) sample is quite regular. Furthermore, the lateral coherence length of the surface state is at least a few times of the terrace width, 12 Å. This is consistent with the value of 20–30 Å reported previously by Kevan, who determined it by measuring the broadening of the (111) surface-state peak in the photoemission spectra as a function of the photoelectron emission angle.[3]

II. EXPERIMENTAL DETAILS

The Cu(332) sample was aligned with Laue x-ray backscattering. The surface was then mechanically polished in this orientation to a mirror finish and finally electropolished in a 59% phosphoric acid solution to expose a mechanical damage-free surface.[7] After introduction into the photoemission chamber, with a base pressure of 1×10^{-10} Torr, the sample was cleaned with repeated cycles of Ar-ion sputtering and annealing at 500 °C. Auger electron spectroscopy was periodically used to verify the sample cleanliness. After a final sputter cycle, the sample was found to remain clean for many hours. The surface structure was inspected with high-energy electron diffraction (HEED) with a 10-keV electron-beam energy.

The photoemission experiment was performed at the Synchrotron Radiation Center of the University of Wisconsin-Madison. Photons of energy 22 eV were used (the reason for choosing this energy will be discussed below). A hemispherical analyzer with a full acceptance angle of 3° was used to collect and analyze the photoemitted electrons. The photoemission geometry is shown in Fig. 1. The sample normal direction, Cu[332], lies along the z axis; the x and y axes are parallel to Cu[$\bar{1}$10] and Cu[$\bar{1}\,\bar{1}$3], respectively. Thus, the Cu[111] direction is tilted at a polar angle of 10° from the sample normal in the direction of the y axis. The position of the analyzer input was varied in order to determine the band dispersion curves. The angle of incidence of the photon beam is 60° within the xz plane ($\theta_I=60°$ and $\phi_I=180°$).

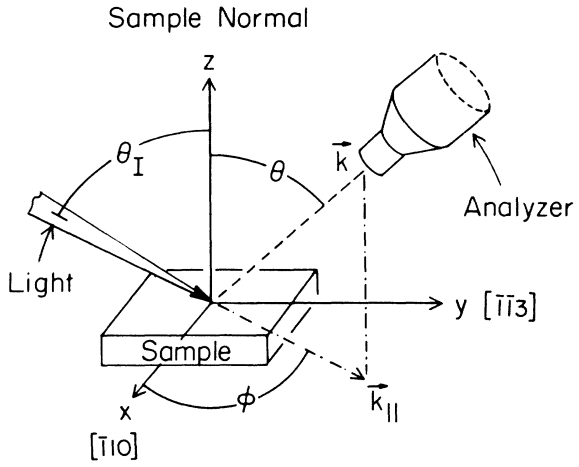

FIG. 1. Photoemission geometry.

III. RESULTS

A. HEED and surface structure

Figure 2(a) shows the expected surface atomic configuration for an ideal Cu(332) face.[8] The shaded circles denote atoms at the step edges, which lie along lines parallel to the [$\bar{1}$10] direction. The [$\bar{1}\,\bar{1}$3] direction also lies in the (332) surface plane and points "up" the steps. Each terrace face consists of a single layer of atoms in a Cu(111) plane. A surface unit cell is indicated by the dashed lines.

HEED patterns were taken from the clean Cu(332) surfaces in a glancing geometry. Schematic representations of the observed HEED patterns are shown in Figs. 2(b) and 2(c) for incident electrons approximately along the [$\bar{1}\,\bar{1}$3] and [$\bar{1}$10] directions, respectively. Based upon comparisons with HEED patterns taken from a Cu(111) sample, the spacings between adjacent lines in the Cu(332) HEED patterns can be shown to be consistent with a Cu sample having the structure shown in Fig. 2(a). The intensities of adjacent lines in the pattern in Fig. 2(b) alternate between bright and dim as indicated with the thick and thin lines, respectively; the center line is a dim line. This effect is not, however, observed in HEED studies of the Cu(111) surface; therefore, the intensity modulation is related to the (332) surface structure. The other HEED pattern, in Fig. 2(c), consists of groups of finely spaced lines which are a result of the broad steps. It can be approximately described as the Cu(111) pattern with additional satellite diffraction lines due to the periodic terrace structure. Overall, the patterns were quite bright with excellent contrast and a number of Kikuchi lines were observed. The sharpness of the satellite lines indicates that the terrace structure is fairly well ordered.

B. Photoemission

Figure 3 shows a set of angle-resolved photoemission spectra for various polar angles θ in the yz plane ($\phi=90°$) shown in Fig. 1; therefore, the analyzer input is along Cu[332] for $\theta=0°$ and along Cu[$\bar{1}\,\bar{1}$3] for $\theta=+90°$. Each spectrum shows the photoemission intensity as a function of the binding energy measured relative to the Fermi level E_F. Intensities of the different spectra in the set were arbitrarily scaled to produce the stack plot shown. In all of these spectra, one peak is observed in the energy range shown superimposed upon an edge at the Fermi level; intense Cu d-band peaks are observed at larger binding energies outside this range. Because there are no known bulk-related peaks located within the range shown,[5] the observed peak must be derived from a surface state. The peak shows significant dispersion as a function of θ; it appears to have the largest intensity and the largest binding energy in the spectra taken with $\theta=6°-8°$. As the surface state disperses towards the Fermi edge, the peak intensity decreases; due to overlapping with the Fermi-edge emission, the peak position becomes difficult to locate.

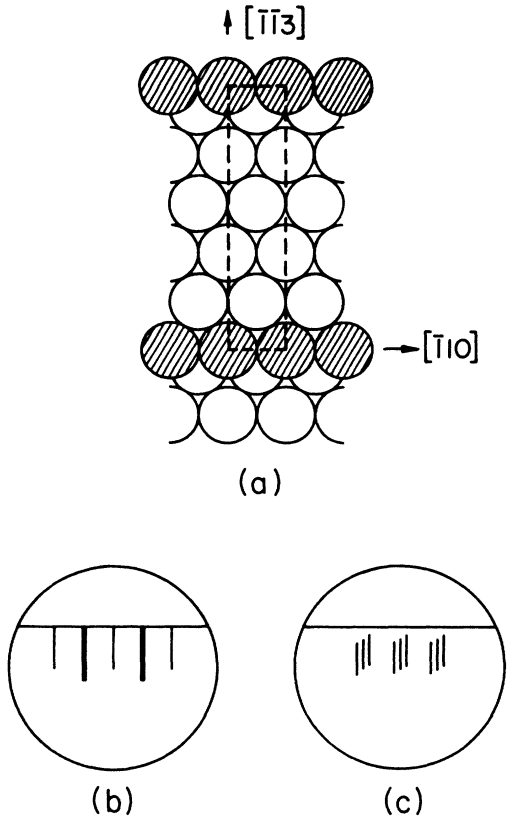

FIG. 2. (a) Expected surface atomic configuration for an ideal Cu(332) stepped surface. The shaded circles denote atoms at the step edges, which lie along lines parallel to the [$\bar{1}$10] direction. The [$\bar{1}\,\bar{1}$3] direction also lies in the (332) surface plane and points "up" the steps. Each wide step face consists of a single layer of atoms in a Cu(111) plane. A primitive surface unit cell is indicated by the dashed lines. (b) Schematic representation of the observed HEED pattern for incident electrons approximately along the [$\bar{1}\,\bar{1}$3] direction. (c) Same as (b) except that the electron beam is approximately along the [$\bar{1}$10] direction.

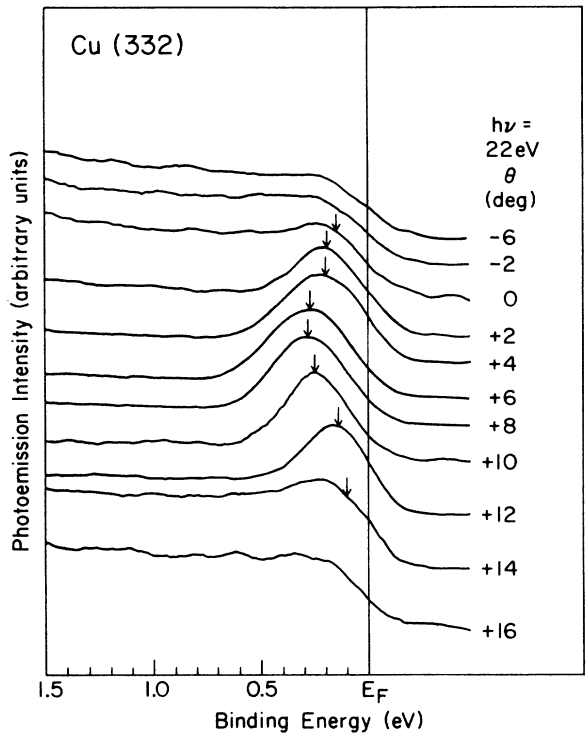

FIG. 3. Angle-resolved photoemission spectra taken with a photon energy of 22 eV from Cu(332). The polar emission angles θ are indicated. The azimuthal angle is $\phi = 90°$ for all spectra. Peak positions are marked with arrows. The binding energies are referred to the Fermi level E_F.

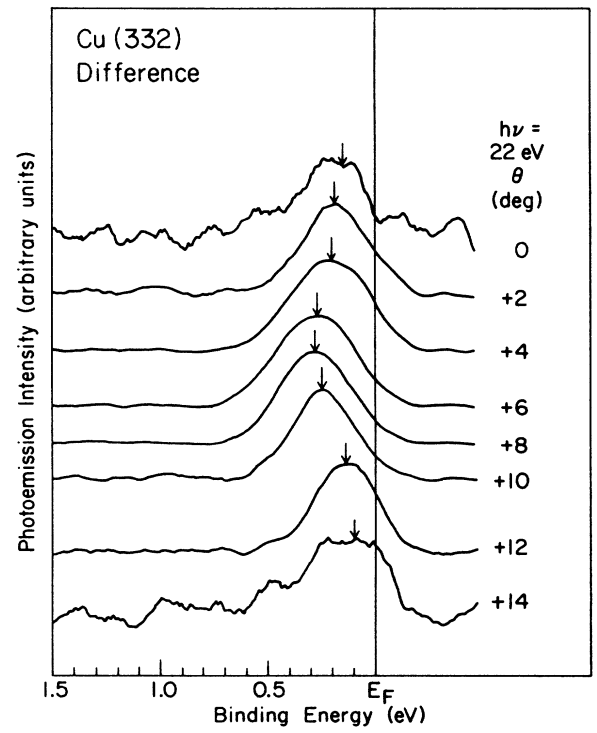

FIG. 4. Difference spectra obtained by subtracting the spectra shown in Fig. 3 by a spectrum taken with a large polar emission angle where the surface state contribution is negligible.

Figure 4 shows a set of difference spectra which were generated by subtracting the spectra in Fig. 3 by a spectrum taken with a large θ where the surface-state contribution is negligible. The purpose of the subtraction is to minimize the Fermi-edge contribution, such that the peak positions can be more easily located. The subtraction method is expected to be reasonably accurate for spectra where the peak and Fermi edge do not overlap significantly; as the peak approaches the Fermi edge, the accuracy decreases and larger uncertainty values have been accordingly assigned to the measurements.

From the peak positions, the two-dimensional band dispersion of the surface state has been determined; the results are displayed in Fig. 5. Each data point indicates the binding energy of the peak as a function of the wave-vector component parallel to the surface $k_{\parallel}$. The polar angle θ describing the analyzer position is also indicated along the upper edge of the figure. The error estimates for both the binding energy and the polar angle are indicated.

The observed dispersive behavior of the surface state somewhat resembles that of the Cu(111) L-gap surface state with the obvious exception that the maximum bind-

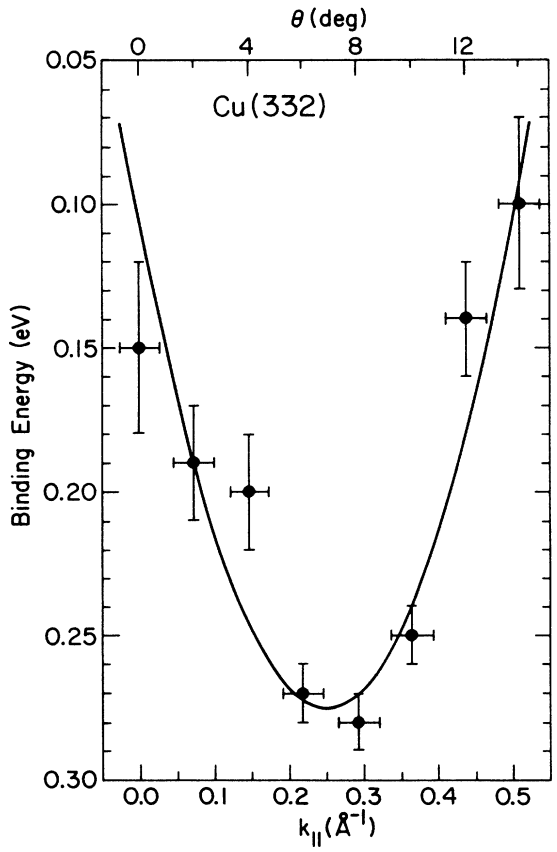

FIG. 5. The two-dimensional band dispersion of the surface state determined from the spectra in Fig. 4. Each data point (solid circles) represents the binding energy of a peak as a function of $k_{\parallel}$. All binding energies are referred to the Fermi level. The polar emission angle θ is indicated along the upper scale. The solid curve is a numerical best fit of a parabola to the data.

ing energy of the Cu(332) feature does not occur at the two-dimensional surface zone center ($\theta=0°$). To determine the value of $k_{\parallel}$ for which the maximum binding energy occurs, the data in Fig. 5 are fitted to a parabola, which is shown by the solid curve. The fit falls within the error range of all but one of the data points. The equation describing the fit is

$$E_B=-2.69(k_{\parallel}-0.25)^2+0.28\ , \tag{1}$$

where $k_{\parallel}$ is measured in units of Å^{-1} and E_B is measured in units of eV. On the basis of the fit, the maximum binding energy of the Cu(332) feature is $E_B=0.28$ eV and it occurs near a value of $k_{\parallel}=0.25\ \text{Å}^{-1}$ (or about $\theta=7°$). It should be noted that the dispersion curve may not be described accurately by a parabolic function; in other words, higher-order terms may be important.[4,9] Therefore, the significance of the coefficient of the quadratic term in Eq. (1) should not be emphasized. But just for the purpose of locating the point of maximum binding energy, this procedure should give a fairly accurate result.

IV. DISCUSSION

The Cu(332) surface feature has two potential origins: the numerous (111) terraces acting independently or the (332) surface as a whole. If the (111) terraces independently support Cu(111) surface states, the contributions from the different terraces will add incoherently. In this case, the observed surface state should be expected to show dispersion curves the same as those of the Cu(111) surface state (with extra broadening due to the finite terrace sizes). In particular, the maximum binding energy should occur along the [111] direction. Figure 5 shows that the maximum binding energy occurs at $\theta=7°$, which is different from the [111] direction at $\theta=10°$. The difference is larger than the overall angular uncertainty estimated to be about 1°. Furthermore, the maximum binding energy and the dispersion of this peak are significantly different from those for the Cu(111) case. Evidently, the terraces do not act independently.

The Cu(332) peak is thus a surface state associated with the (332) surface as a whole. However, since it exists in the bulk L gap, it must have the same origin as the L-gap surface state in the Cu(111) surface.[4] The reciprocal surface net of Cu(332) is a rectangular lattice with lattice parameters equal to 2.46 and 0.524 Å^{-1} along the $[\bar{1}10]$ and $[\bar{1}\,\bar{1}\,3]$ directions, respectively (see Fig. 2); the corresponding primitive surface reciprocal-lattice vectors are just the projection of the bulk reciprocal-lattice vectors $(4\pi/a)(1,2,1)$ and $(2\pi/a)(1,1,1)$ onto the (332) surface. The Cu(332) surface state has a maximum binding energy at about $k_{\parallel}=0.25\ \text{Å}^{-1}$ as noted above. Within experimental accuracy, this value agrees with the distance from the surface zone center to the zone boundary along the $[\bar{1}\,\bar{1}\,3]$ direction, $0.26\ \text{Å}^{-1}$. In other words, the maximum binding energy occurs at the surface zone boundary. This behavior confirms the assignment of the origin of the surface state since the L-gap surface state is expected to have the maximum binding energy at a $\mathbf{k}_{\parallel}$ value equal to the surface projection of the bulk wave vector $(\pi/a)(1,1,1)$ connecting the Γ and L points in the bulk Brillouin zone. For comparison, the surface projection of this wave vector is zero for the (111) surface, and the maximum binding energy occurs right at the surface zone center for this surface.[4]

Even though the Cu(332) surface-state dispersion is different from that of the (111) surface state, the photoemission intensity of the (332) surface state follows rather closely the behavior of the (111) surface state. Thus, the polar angle of about 7° at which the maximum intensity of the (332) surface state occurs is only 3° away from the [111] direction at which the (111) surface state on a (111) crystal attains its maximum intensity. We searched for the (332) surface state in the second surface Brillouin zones by moving the polar angle of the analyzer to $\theta>16°$ and $\theta<-6°$, but did not find significant emission intensity. Thus, considering the regular atomic steps on the (332) surface as a perturbation to the (111) surface, the steps do not cause a significant redistribution in photoemission intensity through umklapp transitions. This is perhaps not surprising because there is only one step for every 5–6 atomic rows.

The peaks seen in Figs. 3 and 4 are rather wide. From an analysis of the Fermi-edge emission at large polar angles θ for which the surface-state contribution is negligible, the total instrumental resolution is about 0.25 eV. Taking into account the finite angular resolution, the peak width is still significantly larger than what is expected. We suspect that the wide width is a result of imperfections in the sample terrace structure. The imperfections may include a small overall misalignment of the sample and slight waviness of the surface after electropolishing, which would cause a finite distribution of terrace width and the formation of kinks. Even for a perfectly aligned planar surface, the presence of imperfections in the terrace structure is not unexpected after the sample is sputtered and annealed. The imperfections can cause an effective broadening of the parallel components of the wave vector, which in turn leads to an energy broadening.

Spectra for other photon energies as well as other geometries, including a scan within a plane containing the Cu$[1\bar{1}0]$ direction, have been taken. These data do not provide any additional important information concerning the surface state, and hence are not included for presentation here. However, the measured angular dependence does provide an additional independent verification of the angular accuracy of this experiment. We now explain why the photon energy of 22 eV was chosen for the set of data presented here. The effect of the finite angular acceptance angle on the momentum broadening can be minimized by using lower photon energies. The surface-state cross section also increases rapidly for decreasing photon energies. In addition, the grating monochromator used in this experiment will have a much better energy resolution at lower energies. Therefore, for higher signal intensity and overall resolution, it would seem to be desirable to use photon energies lower than 22 eV. However, there is a tradeoff. As the photon energy is reduced, the polar emission angle for reaching

the surface zone boundary increases, and can become very close to the angle of 10° between [332] and [111]. For example, with a photon energy of 11.8 eV (Ar resonance line), the polar angle θ would be about 11° for reaching the surface zone boundary where the surface state attains its maximum binding energy. Since the difference between this polar angle and the angle between the [111] and [332] directions is the main indication of whether the surface state is (332) or (111) in nature, it is necessary to use a sufficiently high photon energy to provide an unambiguous differentiation. The 22-eV photon energy provides a 3° difference, and is a good compromise.

V. SUMMARY

To summarize, HEED and angle-resolved photoemission were used to examine a stepped surface, Cu(332). The HEED studies indicated that the surface is composed of fairly regularly spaced steps. A feature with the expected characteristics of an L-gap surface state was observed just below the Fermi edge in the photoemission spectra. The two-dimensional dispersion of this surface state was determined, which is significantly different from the corresponding dispersion curve for the Cu(111) L-gap surface state. Thus, the surface state is delocalized in the surface plane, and its lateral coherence length is larger than the terrace width such that neighboring terraces on the (332) surface cannot be considered as independent. As expected, the maximum binding energy of the (332) surface state occurs at a point on the surface zone boundary, which is defined by the surface projection of the bulk wave vector connecting the Γ and L points in the bulk Brillouin zone.

ACKNOWLEDGMENTS

This material is based upon work supported by the National Science Foundation under Contract No. DMR-8614234. Some of the equipment used for this research was obtained with grants from the National Science Foundation (Grant No. DMR-8352083), the IBM Research Center (Yorktown Heights), the E. I. du Pont de Nemours and Company, the 3M Company, and the Hewlett Packard Laboratory. The Synchrotron Radiation Center of the University of Wisconsin-Madison is supported by the National Science Foundation under Contract No. DMR-8020164. We acknowledge the use of central facilities of the Materials Research Laboratory of the University of Illinois, which is supported by the Department of Energy, Division of Materials Sciences, under Contract No. DE-AC02-76ER01198, and the National Science Foundation under Contract No. DMR-8020250.

---

*Present address: IBM, Hopewell Junction, NY 12533-0999.

[1]H. Wagner, in *Solid State Physics,* Vol. 74 of *Springer Tracts in Modern Physics,* edited by G. Hohler (Springer-Verlag, New York, 1979), pp. 151–221.

[2]P. O. Gartland and B. J. Slagsvold, Phys. Rev. B **12**, 4047 (1975).

[3]S. D. Kevan, Phys. Rev. Lett. **50**, 526 (1983).

[4]N. V. Smith, Phys. Rev. B **32**, 3549 (1985).

[5]R. Courths and S. Hufner, Phys. Rep. **112**, 53 (1984).

[6]A. P. Shapiro, A. L. Wachs, and T.-C. Chiang, Solid State Commun. **58**, 121 (1986).

[7]W. J. McG. Tegart, *The Electrolytic and Chemical Polishing of Metals* (Pergamon, London, 1956).

[8]J. F. Nicholas, *An Atlas of Models of Crystal Surfaces* (Gordon and Breach, New York, 1965).

[9]T. C. Hsieh, P. John, T. Miller, and T.-C. Chiang, Phys. Rev. B **35**, 3728 (1987).